Available online at www.sciencedirect.com

SciVerse ScienceDirect

Procedia CIRP 9 (2013) 29 – 34

www.elsevier.com/locate/procedia

2nd CIRP Global Web Conference

Time-Efficient Prediction of the Surface Layer State after Deep Rolling using Similarity Mechanics Approach

Daniel Trauth[a]*, Fritz Klocke[a], Patrick Mattfeld[a], Andreas Klink[a]

[a]*Laboratory for Machine Tools and Production Engineering (WZL) of RWTH Aachen University, Steinbachstr. 19, 52062 Aachen, Germany*

* Corresponding author. Tel.: +49 241 80 27999; Fax: +49 241 80 22293. *E-mail address*: D.Trauth@wzl.rwth-aachen.de.

Abstract

Highly stressed components like turbine blades made of IN718 (ASTM: B637), crankshafts made of 42CrMo4 (ASTM: A322-4140) or connecting rods made of GGG60 (ASTM: A536-80-55-06) have to satisfy stringent requirements regarding durability and reliability. The induction of compressive stresses and strain hardening in the surface layer of technical components has proven to be a promising method to significantly increase the fatigue resistance. These required surface layer properties can be achieved by deep rolling. The determination of optimal deep rolling process parameters still requires elaborate experimental set-up and subsequent time- and cost-intensive measurements. Therefore, this work provides a new approach to determine surface layer properties by applying similarity mechanics in combination with FE-simulation of the deep rolling process. Thereby, this approach provides an efficient estimation of process results in which time-costly and challenging FE-simulations become redundant.

Selection and peer-review under responsibility of International Scientific Committee of the 2nd CIRP Global Web Conference in the person of the Conference Chair Dr. Sotiris Makris

Keywords: Deep Rolling; Residual Stresses; Strain Hardening; Similarity Mechanics; Prediction; Finite Element Method

1. Introduction

Highly stressed components like turbine blades made of IN718, crankshafts made of 42CrMo4 or connecting rods made of GGG60, have to satisfy stringent requirements regarding durability and reliability. The induction of compressive stresses and strain hardening in the surface layer of technical components has proven as to be promising method to significantly increase the fatigue resistance [1-3]. These surface layer properties can be achieved by deep rolling. Compared to alternative mechanical strain hardening processes like shot-peening or laser-peening, deep rolling distinguishes itself by three substantial advantages. Firstly, the highest and the deepest compressive residual stress state can be induced to the components surface layer [4]. Secondly a high strain hardening, especially deep underneath the surface layer, is evolved by deep rolling [5]. This can additionally be increased by the variation of rolling parameters [6]. The third major advantage of deep rolling is the improvement of the surface quality, especially in comparison to the shot-peening process. Shot-peening causes a keying of the surface, which could also result in a downgrading of the fatigue strength [4,7].

The substantial disadvantage of deep rolling is the complex determination of suitable process parameters. It is currently based on elaborate experimental set-up and subsequent time- and cost-extensive measurements. In recent works the Finite Element Analysis (FEA) was applied to predict the deep rolling influence on the surface layer and to thereby enable a time and cost efficient process design [8]. Whereas the FEA-based approach delivers a quantitative estimation of the induced residual stresses and strain hardening into the surface layer, for an accurate process modeling still a high expertise of the user as well as high computation time are required. These disadvantages inhibit the wide application of the deep rolling process in the industrial environment. For these reasons, a new method is required, which enables an efficient and also industrially applicable process design.

The theory of mechanical similarity fulfills these requirements. This method is widely used in fluid mechan-

Selection and peer-review under responsibility of International Scientific Committee of the 2nd CIRP Global Web Conference in the person of the Conference Chair Dr. Sotiris Makris
doi:10.1016/j.procir.2013.06.163

ics for the description and modeling of highly complex and dynamic physical correlations of fluids [9]. A more specific application of the similarity mechanics for incremental forming processes can be found in [10]. Hergemoeller applied this method in combination with experimental and simulated input data to enable an accurate and efficient process design of the shot peening process.

Since it could be principally shown that an approach based on similarity mechanics can provide an accurate and very efficient method for the determination of the correlation of process parameters and their influence on the process results, in this paper the applicability of the similarity mechanics will be extended to the deep rolling process. Based on process results obtained from verified FE-models, a new similarity mechanics model will be developed for the deep rolling process.

2. Experimental Examination of Deep Rolling

Deep rolling is characterized by numerous process input parameters. To determine the significance of these parameters for the examined materials and geometries experimental trials on a special designed analogy specimen were carried out based on a full factorial design according to Design of Experiments (DoE).

2.1. Experimental set-up

The experiments were executed and supervised by ECOROLL AG Werkzeugtechnik, Celle, Germany. The trials were carried out by a variation of the process parameters: deep rolling pressure ($p = 100; 400$ bar), deep rolling ball diameter ($d = 6; 13$ mm), the overlap between two deep rolling lanes ($o = 30; 80\%$), deep rolling velocity ($v = 70; 150$ mm/s) as well as the geometry (lateral surface area, outer radius, borehole) and workpiece material (IN718, 42CrMo4, GGG60). All 144 deep rolling experiments were executed with the hydraulic deep rolling tools HG6 and HG13, a hydraulic power unit HGP 400 and a conventional CNC lathe.

Process output parameters: Residual stresses in depths up to 0.5 mm were measured every 20 µm by means of the incremental hole drilling method, which is commonly used for the determination of in-depth non-uniform residual stress states [11]. In order to calculate the residual stress corresponding to the measured strain, a developed equipment by MTU Aero Engines was applied, using the integral evaluation method and a Ti-Al-Ni plated tungsten-carbide-driller with a diameter of 0.8 mm. Residual stresses were measured parallel and perpendicular to the rolling direction.

In order to characterize the strain hardening state after deep rolling, microhardness measurements (HV0.1) were carried out using a Fischerscope microhardness measurement device. To support the evaluated data, the macrohardness (HRC) was determined as well. The surface roughness parameter measured according to DIN EN ISO 4287:1998 is the arithmetic Roughness R_a.

2.2. Identification of significant process parameters

The evaluation of the process output parameters according to the rules of DoE show different characteristics due to different material properties (see exemplarily for residual stresses in Figure 1). Table 1 summarizes all significant process parameters for each output parameter. The significance within a row decreases from left to right. The sign indicates the direction in which this parameter has to be changed so that the residual stresses and the strain hardening are maximized and the surface roughness is minimized:

Table 1. Overview of the significant process parameters

Output parameter	IN718	42CrMo4	GGG60
Residual stresses	$p+, o+, v-$	$p+, d+, v-$	$p+, d+, o+$
Strain hardening	$p+, d+, v-$	$p+, d-, o+$	$p+, d+, o-$
Surface roughness	$d-, p-, o-$	$d+, o+, v+$	$p-, d-, v+$

3. FE-Modeling of the Deep Rolling Process

A process model connects the process input parameters with the process results correctly using a phenomenological and causal approach. This can be achieved qualitatively by explanatory models derived from basic process understanding or quantitatively by numerical modeling. In this section, the development of a numeri-

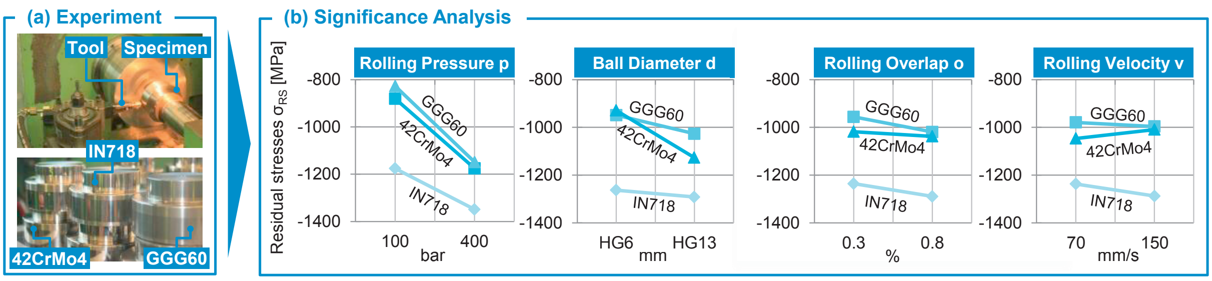

Figure 1: Experimental set-up (a) and results of the significance analysis for the process output parameter residual stresses (b)

cal model based on the finite element method (FEM) is described. This chapter explains the 3D model development exemplarily for the lateral surface area of an axially symmetric part. Simulation models for boreholes and outside radii were created as well.

3.1. Model development

The FE-models were developed in Simulia Abaqus 6.12. Because of numerous nonlinearities in contact mechanics and process kinematics the explicit solver suitable for dynamic problems was chosen. In deep rolling of axially symmetric parts, typically the workpiece rotates around its own axis while the deep rolling tool conducts translational movements as in turning. To increase the numerical stability and to reduce the computation time of the FE-models, special modification regarding process kinematics and the numerical set-up have been made.

The transfer of the rotational movement of the workpiece to the deep rolling tool allows fixing the deformable workpiece. Fixed deformable bodies are most suitable for a special modeling technique called “mass scaling”. Mass scaling increases the critical time increment in explicit simulations, which reduces significantly the computation time. Numerical simulations have shown that a mass scaling factor of 250 for the whole FE-model has no impact on the process output parameters and is therefore chosen for further analyses. By this the computation time of one simulation is decreased by one-third.

Additionally to decrease the computation time only a representative cut-out of the axially symmetric parts was investigated. To optimize contact mechanics while deep rolling in order to avoid mechanical oscillations of the deep rolling tool, process kinematics were modeled by the help of a mass-spring-damper-system. The spring characteristic was approximated with the elastic material definition of the investigated workpiece material. The mass and deep rolling forces were derived from experimental trials. The damping factor was then determined analytically so that the system is critically damped, which means no over- or under-damping occurs during the indentation of the tool. This allows minimizing the length of the cut-out model since from the start the system achieves its equilibrium as quickly as possible without oscillating.

To evaluate the process output parameters after deep rolling simulation, a special designed mesh with evaluation-paths was implemented. The deformable workpiece was modeled in 3D using hexagonal continuum elements with reduced integration, neglecting thermal effects according to [4]. Hexagonal elements qualify to define straight nodal paths from the oudside of the workpiece into the surface layer. A fine mesh (axial seed of 100 µm, radial and tangential seed of 50 µm) ensures a high resolution of the investigated surface layer to a depth of 0.5 mm. To minimize numerical rounding errors and numerical singularities, 9 nodal paths were placed around the geometric center of the surface layer to be evaluated and then averaged.

3.2. Material definition

The process output parameters strongly depend on the modeled material properties. To model the material characteristics as precisely as possible, especially the Bauschinger effect, experimental stress-strain-tests under cyclic loading with maximum strains of 2%, 4% and 6% elongation were carried out at the Institute for Applied Materials IAM–WK of Karlsruhe Institute of Technology (see Figure 2 (a)). The material characteristic was numerically described using a combined cyclic nonlinear isotropic and kinematic plasticity model, referred to as the constitutive Lemaitre-Chaboche-Plasticity-Model (LCP model) [12]. The isotropic hardening component in the LCP model is controlled by,

$$\sigma^0 = \sigma_0 + Q_\infty \left(1 - e^{-b\cdot\varepsilon^{pl}}\right) \tag{1}$$

where σ^0 is the instantaneous yield surface size, σ_0 is the initial yield surface size and Q_∞ and b are material parameters. The kinematic hardening component is described by a modified Ziegler law which considers the nonlinear response. Under conditions of an uniaxial stress state, the reduced scalar equation is given by

$$\dot{\alpha} = C\dot{\varepsilon}^{pl}\frac{(\sigma-\alpha)}{\sigma^0} - \gamma\alpha\dot{\varepsilon}^{pl} \tag{2}$$

where $\dot{\alpha}$ is the incremental change in the backstress

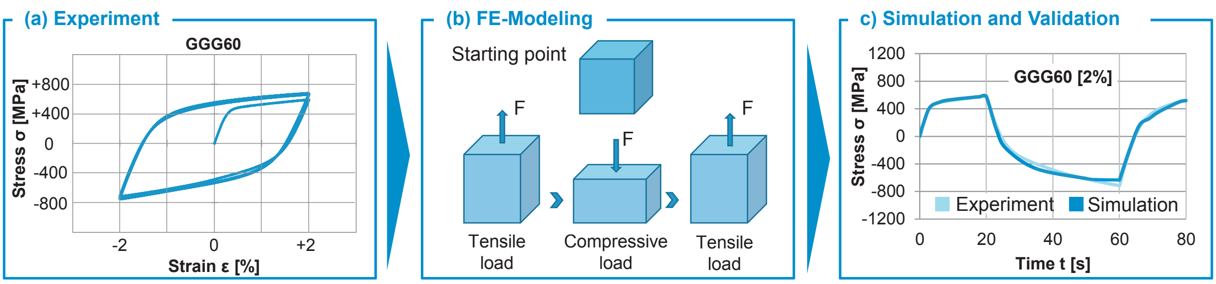

Figure 2: Result of a cyclic stress-strain-test at 2 % elongation (a); numerical set-up (b) and determination of the LCP model parameters (c)

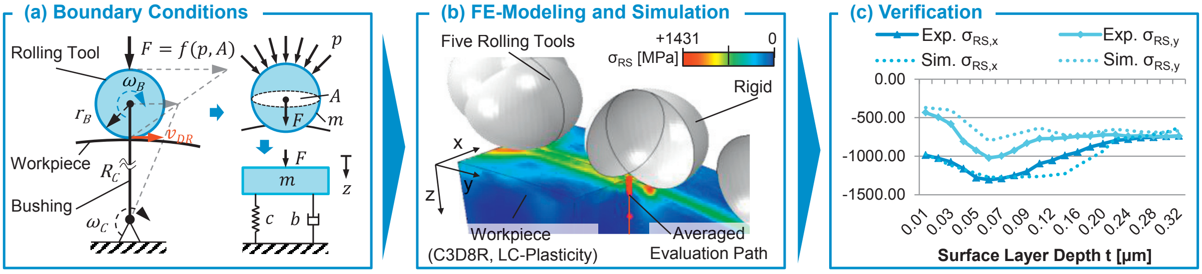

Figure 3: Analysis of the boundary conditions (a); FE-modeling of the overlap (b) and validation of the simulated deep rolling process (c)

tensor α and C and γ are material parameters. The material parameters Q_∞, b, C, γ were determined by conducting a regression analysis (see Figure 2 (c), Table 2).

Table 2. Material parameters of the constitutive LCP model

Material property	IN718	42CrMo4	GGG60
Young's Modulus E [MPa]	200000	207000	169500
Poisson ratio ν [-]	0.284	0.29	0.275
Density ϱ [kg/dm³]	8.2	7.2	7.7
Initial yield stress σ_0 [MPa]	1132	813	402
Isotropic parameter Q_∞ [-]	160	160	150
Isotropic parameter b [-]	20	5	10
Kinematic parameter C [-]	20300	50000	30000
Kinematic parameter γ [-]	70	190	140

3.3. Boundary conditions

Contact modeling: For modeling the interaction between a deformable workpiece and rigid tools that may move, the finite-sliding formulation of contact pairs, where separation and sliding of finite amplitude and arbitrary rotation of the surfaces may arise, was used.

Friction modeling: The friction was modeled using an extended version of the classical isotropic Coulomb friction model. The extensions include an additional limit on the allowable shear stress. If the equivalent stress exceeds the stress limit, slip can occur. Thereby, the friction model is able to consider stick-slip-effects, which can occur during deep rolling at high pressures.

Model kinematics: In order to consider the influence of the surrounding material to the simulated cut-out of the workpiece geometry the boundary conditions on the workpiece are defined as encastre and symmetry planes. Research results showed that a complete fixation of the lateral faces of the model leads to residual stress elevation and an assumption of unconstrained lateral faces leads to reduced stresses. Thereby, the use of symmetry planes is the most accurate possibility for the simulation of the surrounding material behavior. The tool kinematics are described by three different boundary conditions: *Indentation* of the rolling tool normal to the workpiece surface, *rotatory movement* and *translational movement* along the workpiece axis. The pressure applied on the workpiece is substituted by definition of a corresponding tool *indentation force*. This substitution enhances the stability and robustness of the simulation, and reduces the computation time considerably. The deep rolling force was determined analytically and experimentally. It was detected that the deep rolling force can be approximated by the product of the hydraulic deep rolling pressure p applied by the hydraulic system and the projected cross section A of the deep rolling ball (see Figure 3 (a)).

Since the *rotatory movement* of the workpiece is transferred to the deep rolling tool, the kinematics of the tool have to ensure the relative rotation of the deep rolling ball around the own axis rolling up on the workpiece surface as well as the angular rotation around the workpiece axis. The kinematic system is modeled in Abaqus using two multi-point-connectors of type pin and one bushing connector. The bushing connector is defined as a rigid beam, but with the exception, that the length of the bushing connector is radially variable. When the deep rolling force is applied, the bushing connector adapts itself automatically on the workpiece geometry. The above mentioned mass-spring-damper-system is realized by the bushing connector properties.

To avoid a relative acceleration of the deep rolling ball during the indentation, an initial angular velocity for the ball was defined using the initial condition option and was determined by the equation (Figure 3 (a))

$$\omega_B = \frac{v_{DR} \cdot \left(1 + \frac{r_B}{R_C}\right)}{r_B} \tag{3}$$

where r_B is the radius of the deep rolling ball, R_C is the length of the bushing connector representing the workpiece diameter and v_{DR} is a given deep rolling velocity.

The *translational movement* of the deep rolling tool was modeled using multiple deep rolling balls. The ball offset f was determined using the equation

$$f = (1 - o) \cdot b \tag{4}$$

where b is the width of one single deep rolling lane and o a given overlap for multiple deep rolling lanes. To achieve that the multiple use of tool balls has no inadvertent influence on the process output parameters, the tool balls were started in sequence with a delay of half the process time for a single lane (see Figure 3 (b)).

3.4. Verification of the FE-model

By help of the earlier mentioned nine evaluation paths the residual stresses parallel and perpendicular to the deep rolling lane and the strain hardening were determined and averaged in the middle of the deep rolled surface and compared to the experimental results. According to [4] strain hardening was evaluated by means of the equivalent plastic strain (PEEQ) while the residual stresses are described by the von-Mises-stress-tensor (S). Figure 3 (c) shows a very good accordance of the numerical residual stress with the experimental measured stress. Thus the FE-model is verified and qualifies for further investigations using similarity mechanics.

4. Prediction of the Surface Layer State using Similarity Mechanics Approach

Since experimental trials are costly and time-intensive, they can only provide results for a limited number of process parameters. Numeric simulations are a more efficient approach to expand the examined number of parameters, yet the complete field of applicable parameters cannot be covered. For an efficient process design a method is required, which enables the possibility to cover the entire correlation between process parameters and process results. In this context a promising approach to meet this requirement is provided by the application of similarity mechanics.

4.1. Process design and characterization of output values

A typical residual stress depth profile $\sigma(z)$ is shown in Figure 4 (a). $\sigma(z)$ is characterized by four significant values: the residual stress at the surface σ_0 $(z = 0)$, the minimum residual stress σ_{min} $(z = z_{min})$ and the maximum residual stress σ_{max} $(z = z_{max})$. Additionally the zero crossing point $(z = z_0)$, describing the change of sign from compressive residual stress to tensile residual stress, is important. The knowledge of these characteristic points allows predicting a depth profile for the considered output parameter and is therefore the aim of similarity mechanics.

4.2. Estimation of output values applying analytic functions

In order to estimate the residual stress depth profile for arbitrary combinations of process parameters, a procedure applying similarity mechanics in combination with a product ansatz was applied [9-10]. It establishes analytic functions to describe the correlation between dimensionless input and output variables. The data for establishing the correlation function was derived using the simulation results of the deep rolling process described in chapter 3.

In order to perform a dimensional analysis, all parameters are classified into process, geometry, material, and material model parameters. In total, 19 parameters were determined. According to the Buckingham theorem [13], a dimensionless output value $\sigma(z)$ of a physical problem depends only on $p = n - q$ dimensionless numbers Π_i where n is the number of influencing parameters and q is the rank of the dimension matrix. Considering the three dimensions (length l, time t, mass m), the scaling problem is completely described, when the dependency of all linearly independent dimensionless input values is known for an interesting output value by:

$$\sigma(z) = \bar{a}(\Pi_1, \Pi_2 \ldots \Pi_{p=n-q}). \quad (5)$$

Though similarity mechanics enables a reduction of the input variables, the necessary effort in order to determine equation (5) would still be too extensive for a complex simulation model like the deep rolling model. Therefore a product ansatz [9] is chosen as a further simplification, which requires only the dependencies of one input value:

$$\sigma(z) = K\, \bar{a}(\Pi_1) \cdot \bar{a}(\Pi_2) \cdot \bar{a}(\Pi_3). \quad (6)$$

Here $\bar{a}(\Pi_i)$ with $i = 1 \ldots 3$ represent analytical functions describing the relationship between the dimensionless output value a and the dimensional input value Π_i.

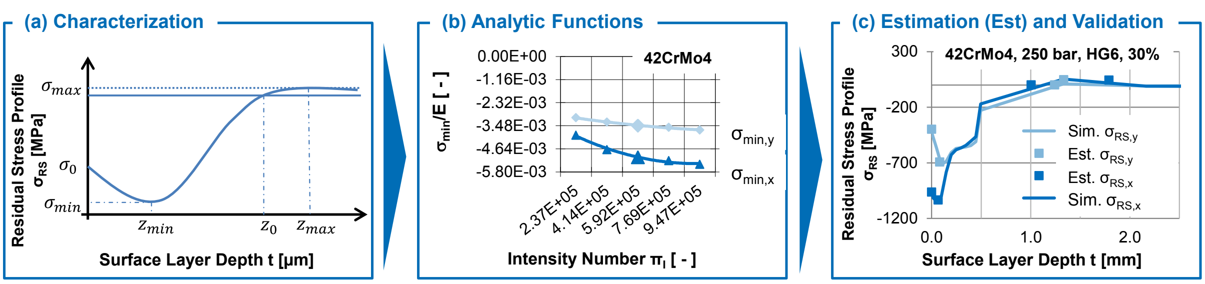

Figure 4: Characterization of a residual stress depth profile (a) and prediction of the significant values using similarity mechanics approach (b, c)

The analytical functions are established based on the simulation data. $K = 1/a_0^2$ represents the dimensionless output value at standard parameters of the deep rolling process.

Based on the significant process parameters from Chapter 2, suitable dimensionless numbers were determined:

Table 3. Suitable dimensionless numbers of deep rolling process

Description	Formula	Description	Formula
Intensity Number	$\Pi_I = p/E$	Geometry Number	$\Pi_G = d/D$
Overlap Number	$\Pi_o = f/D$	Velocity Number	$\Pi_V = v/\sqrt{E/\rho}$

Exemplarily, Figure 4 (b) shows the simulation results at standard parameters and their analytic functions for the dimensionless output value $\sigma_{min}\ (z = z_{min})$. Stresses were related to the Young's Modulus E, depth values were related to the ball diameter d. The benefit of the analytic function is that the results can be described by only one dimensionless value. With a total of 144 analytic functions it is possible to get an estimation of the desired output values for arbitrary input parameters without running further simulations or experiments.

4.3. Validation of the developed model

In order to verify the results of the product ansatz, the output values were compared with the results of FE-simulations. In Figure 4 (c) an example for a graphical output is given. The significant values of a residual stresses profile can be well estimated by the presented method with a maximum deviation of 5%. The authors propose the following function to connect the characteristic values to a representative residual stress depth profile as shown in Figure 4 (a):

$$\sigma_{RS}(z) = \begin{cases} \sigma_{min} - \dfrac{\left(1-\frac{z}{z_{min}}\right)}{(\sigma_{min}-\sigma_0)^{-1}} & ,0 \le z < z_{min} \\ \sigma_{min}\left(\dfrac{1-\frac{(z-z_{min})^2}{(z_0-z_{min})^2}}{\left(1+\frac{(z-z_{min})^2}{(z_0-z_{min})^2}\right)^2}\right) & ,z_{min} \le z < z_0 \\ \sigma_{max}\dfrac{(z^2-z_0^2)}{(z_{max}^2-z_0^2)} & ,z_0 \le z < z_{max}. \end{cases}$$

5. Conclusion and Outlook

The presented approach offers a very effective and simple method to enable an estimation of process results like residual stresses or strain hardening for process parameters using similarity approach. Therefor analytic functions for significant depth profile values have been derived based on validated numerical results. Furthermore the estimation can be improved by evaluating more significant depth profile values.

Future work aims on the prediction of the fatigue life using similarity mechanics. Therefore dimensionless numbers relating the surface layer state to a S/N curve are determined. Using experiments and FE-analyses, suitable analytic functions allow the prediction of the number of stress cycles or the critical fatigue stress depending on residual stresses, strain hardening and the surface quality.

Acknowledgements

The authors would like to thank the German Federal Ministry of Economics and Technology (BMWi) for supporting this research project through the Central Innovation Programme for SME (ZIM). Further, we express our graditute to K. Röttger and S. Fricke of ECOROLL AG Werkzeugtechnik for their support in conducting the experiments cited in this paper.

Reference

[1] Nalla, R., Altenberger, I., Noster, U., Liu, G., Scholtes, B., Ritchie, R., 2003. On the influence of mechanical surface treatments - deep rolling and laser shock peening - on the fatigue behavior of Ti-6Al-4V at ambient and elevated temperatures. Materials Science and Engineering: p. 216–230.
[2] Krull, P., Nitschke-Pagel, T., Wohlfahrt, H., 1999. Influence of shot peening and high pressure water peening on near surface microstructure of 316 Ti stainless steel. In: Brebbia, C., Kenny, J.M.: Surface treatment IV. Computer methods and experimental measurements, p. 291–309.
[3] Wagner, L., 1999. Mechanical surface treatments on titanium, aluminum and magnesium alloys. Materials Science and Engineering: A 263(2):p. 210–216.
[4] Mader, S., 2006. Festwalzen von Fan- und Verdichterschaufeln. PhD thesis RWTH Aachen University.
[5] Prevey, P.S., Shepard, M.J., 2001. The Effect of Low Plasticity Burnishing (LPB) on the HCF Performance and FOD Resistance of Ti-6AI-4V. Proc. 6th National Turbine Engine HCF Conference, Jacksonville, FL, March 5-8.
[6] Röttger, K., 2003. Walzen hartgedrehter Oberflächen. PhD thesis RWTH Aachen University.
[7] O'Hara, P., 1999. Superfinishing and shot peening of surfaces to optimise roughness and stress. In: Brebbia, C., Kenny, J.M.: Surface treatment IV. Computer methods and experimental measurements, p. 321–330.
[8] Klocke, F., 2010. Finite element analysis of the roller burnishing process for fatigue resistance increase of engine components. Proceedings of the Institution of Mechanical Engineers, Part B: Journal of Engineering Manufacture January 1, 2011 vol. 225 no. 1, p. 2-11.
[9] Sedov, L., 1993. Similarity and dimensional methods in mechanics. CRC Press.
[10] Hergemoeller, R., 1982. Anwendung der Ähnlichkeitstheorie auf Probleme der Umformtechnik. PhD thesis RWTH Aachen University.
[11] Kelsey, R., 1956. Measuring non-uniform residual stresses by the hole drilling method. Proc. Soc. Exp. Stress Anal. 14, p. 181–194.
[12] Lemaitre, J., Chaboche, J., Benallal, A., Desmorat, R., 2009. Mécanique des matériaux solides - 3ème édition. Dunod.
[13] Buckingham, E., 1914. On Physically Similar Systems; Illustrations of the use of Dimensional Equations. Phys. Rev. 4(4), p. 345–376.